Modulated thermal wave imaging approach to detect subsurface microcracks and their coalescence in deep mines for rock burst (strain burst) prediction.

Mrityunjay Jaiswal
Department of Civil Engineering, Indian Institute of Technology Ropar, Rupnagar, Punjab, India

Resmi Sebastian
Department of Civil Engineering, Indian Institute of Technology Ropar, Rupnagar, Punjab, India

Ravibabu Mulaveesala
Centre for Sensors, iNstrumentation and cyber-physical Systems Engineering (SeNSE), Indian Institute of Technology Delhi, Hauz Khas, New Delhi

ABSTRACT: Rock burst, which is exceptionally powerful and abrupt, is one of the most dangerous geological hazards in deep mines. Although it is difficult to prevent rock explosions, it can be predicted with continual monitoring. Traditional monitoring systems produce a large quantity of data and false signals. Most methods are affected by blasting and other mining activities. This study used modulated thermal wave imaging to locate the high damage zone in a rock sample containing artificially implanted subsurface microcracks prior to any rock bursting. Finite element (FE) simulations were used to examine the infrared thermal response of a rock sample to a fixed-frequency sinusoidal heat wave. To automate detection, a cutting-edge deep-learning technique was used to identify, localize, and segment cracks. A sizable dataset of images with a resolution of 640×480 was produced for the algorithm training and validation. The F1 score and precision of the applied method were considerably high.

Keywords: Rockburst, thermal monitoring, infrared thermography, deep learning.

1 INTRODUCTION

Resource extraction depth is increasing exponentially as a result of technological advancements and increased demand for ores. When a mine is dug deeper, the most common problem is a rock burst (Budiansky et al. 1976), which occurs quickly and eventually results in the collapse of the entire structure. Sometimes it is so devastating that it won't give the mine workers enough time to escape safely. As a result, research into early rock burst prediction has been ongoing for many years. It is exceedingly challenging to forecast because of the heterogeneity and high confining pressure in the underlying rock. Due to excavation, tensile stress increases in the principal plane of the tunnel, creating microcracks at weak spots (as shown in Figure 1) and softening the entire rock mass (Piane et al.,2015 and Griffiths, L et al., 2017). As these cracks spread, rock bursts occur. Therefore, rock bursts can be projected by continuous monitoring of precursors such as the formation of microcracks or weak spots. Researchers have used various predicting methods based on stresses present on rock (Miao et al., 2016), microcosmic activity (Lu et al., 2012), acoustic emission (He et al., 2010 and He et al., 2019), electromagnetic radiation (Li, Xuelong, et al., 2016) and optics (Luodes et al., 2008).

The traditional methods are contact and point-based methods, and their accuracy is strongly reliant on the accessibility of each and every corner in the region of interest. Furthermore, all of the methods mentioned above are affected by background noise and are associated with significant errors. Therefore, a meticulous non-destructive testing method is demanded to assure the structural integrity of a rock structure in mines and tunnels. As a result, in order to address the aforementioned issue, continuous temperature monitoring is a solution that is currently being employed in a wide range of industries. Every material has its own thermal signatures and whenever any event occurs or some cracks generate, the temperature at that location increases (Guerin et al.,2019) which can be monitored using an infrared thermal camera, which is referred to as, infrared thermography (IRT). Using infrared thermography, it is quite possible to characterize the rock failure stages and location of burst prone zone. Furthermore, Guerin et al., (2019) have used this technique for a rock quality survey by observing the temperature of a rock mass at various time intervals. Due to the exposure to sunlight, the temperature of rocks increases in the daytime and they get cooled down at night. Since every material takes its own time to heat and cool, researchers adopt this method to monitor the exposed rock to investigate the presence of fractures, joints and rock bridges. This method is very advantageous as it is fast, reliable and can be inspected remotely. However, it is a time-consuming method, as one single observation takes a whole day and night and rock masses at deep mines and at deep tunnels are not exposed to sunlight. As a result, the efficacy of active thermography, which involves heating and cooling the rock surface in a specific pattern with external heat, has been examined in this work. Typically, the external temperature application pattern appears in the form of a rectangular pulse, a sinusoidal pulse with a fixed frequency (commonly referred to as lock-in thermography), or a sinusoidal pulse with an encoded variable frequency. However, this particular study illustrates only the responses and feasibility of a fixed-frequency sinusoidal pulse and proposes a post-processing approach to reduce the noises during experiments. A cutting-edge deep learning algorithm has been used for training and validation in order to automate the identification procedure.

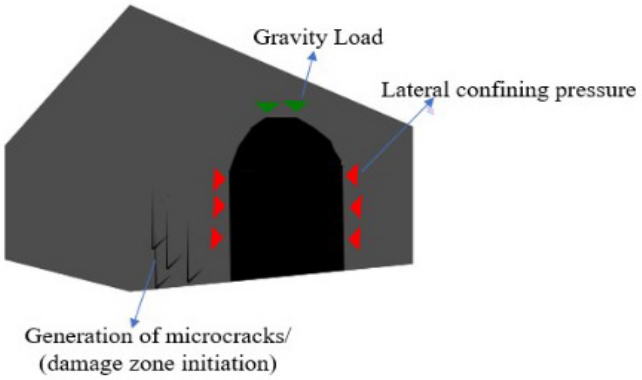

Figure 1. Schematic diagram of the initiation of microcrack zone inside a tunnel.

2 METHODOLOGY

2.1 Simulation of a heat wave

The proposed approach simulates a 3-dimensional granite rock with fabricated cuboid-shaped microcracks; the crack was assumed to have no filler material (see Figure 2). The thermophysical characteristics of the granite and the air inside the crack are displayed in Table 1. The cracks were so positioned that they formed a junction which was the meeting point of one main crack and two wing cracks. Tetrahedral elements were used to create models with a normal mesh to perform numerical simulations using the finite element method (FEM) based application COMSOL®. The mesh density and element count were adjusted through a series of iterations in order to reduce the computing time and truncation error. A standard infrared imaging experiment on a rock sample is illustrated in Figure 3. Heat modulation in the form of a fixed-frequency sinusoidal wave (see Figure

4) was produced using the control module attached therein. The control device additionally synchronizes the thermal infrared camera's frequency of acquisition.

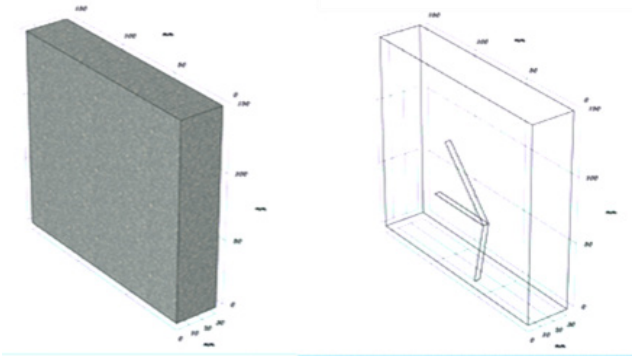

Figure 2. Schematic representation of granite with artificially planted crack.

Table 1. Thermophysical properties of granite and air inside the crack.

Properties	Granite	Air (at 1 atm)
Thermal conductivity, k(W/m.K)	2.9	0.024
Density, ρ(kg/m^3)	2600	1.208
Heat carrying capacity, c (J/kg-K)	850	1006

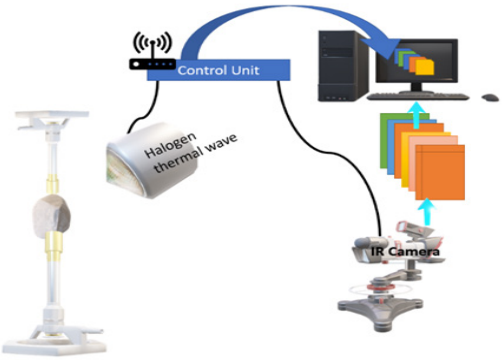

Figure 3. Schematic of the typical infrared thermography experimental arrangement.

The angular frequency of the thermal wave is calculated using the heat diffusion equation as:

$$\frac{\partial}{\partial x}\left(\frac{k_0}{\rho_0 c_0}\frac{\partial T_g}{\partial x}\right)+\frac{\partial}{\partial y}\left(\frac{k_o}{\rho_o c_o}\frac{T_g}{\partial y}\right)+\frac{\partial}{\partial z}\left(\frac{k_o}{\rho_o c_o}\frac{T_g}{\partial z}\right)+\frac{Q}{\rho_o c_o}=\frac{T_g}{\partial t} \quad (1)$$

When, the external boundries were considered as in adiabitic condition and the heat stimulus as a sinosoidal wave, the solution of above equation is,

$$T(Z,t)=\frac{nJ_i}{2e\sqrt{\omega}}e^{\left(\frac{-z}{\mu}\right)+i\left(\omega t-\frac{z}{\mu}\right)} \quad (2)$$

Where Q is the rate at which energy is created as a result of an external heat source, Tg is the spatial temperature of rock at time t, ρ_o is density, c_o is specific heat capacity, and k_r is thermal conductivity. The thermal diffusivity of rock sample, designated as "alpha (α)," is determined by

$$\alpha=\frac{k_o}{\rho_o c_o} \quad (3)$$

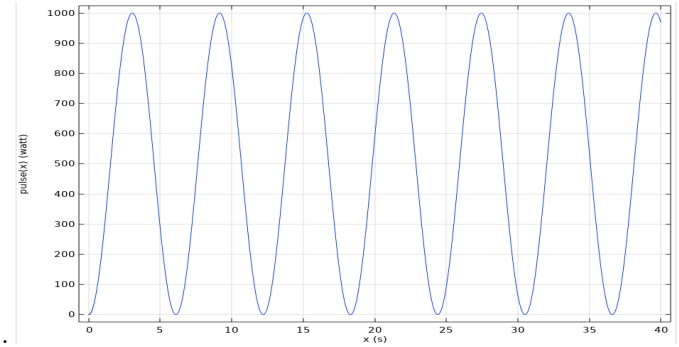

Figure 4. Schematic diagram illustrating the sinusoidal heat stimulus.

The initial temperature was assumed to be 300.15 K, which represents the average room temperature. The subsequent heat reactions over the surface of rock were recorded at a rate of 10 frames per second.

2.2 Post processing

Zero mean thermal gradient: The output thermogram generally has noises from uneven heating, emissivity, or other outside factors. The direct analysis of the thermogram can yield some inaccurate results, hence post processing is required. In order to verify the effectiveness of the recommended technique for detection in the presence of noise, Gaussien noises were added to the thermograms obtained from the simulation. Furthermore, the pixel value of each thermogram which cointains noises were processed using MATLAB to obtain a zero mean pixel curve by polynomial fitting of temporal pixel value (as shown in Figure 5).

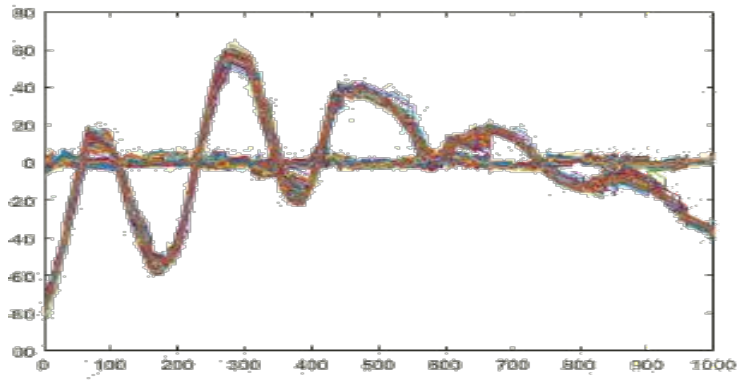

Figure 5. Zero mean pixel profile of thermogram.

3 RESULTS AND DISCUSSION

3.1 Detection potential

Two zones, the high damaged zone and the low damaged zone, were created by dividing the total surface area of the rock. The signal to noise ratio (SNR) was used as a measure of efficiency, and the resulting thermogram and average pixel value for both zones were analysed. The thermogram of granite, which was created from the fitted noisy data, is depicted in Figure 6. Figure 7 illustrate the outcome after processing zero mean to noisy thermal data. It was discovered that the temperature difference between the sound zone and cracked zone is less than 70 mK, implying that the thermal camera needs to be sensitive to temperatures below 70 mK to distinguish between cracks and the sound zone.

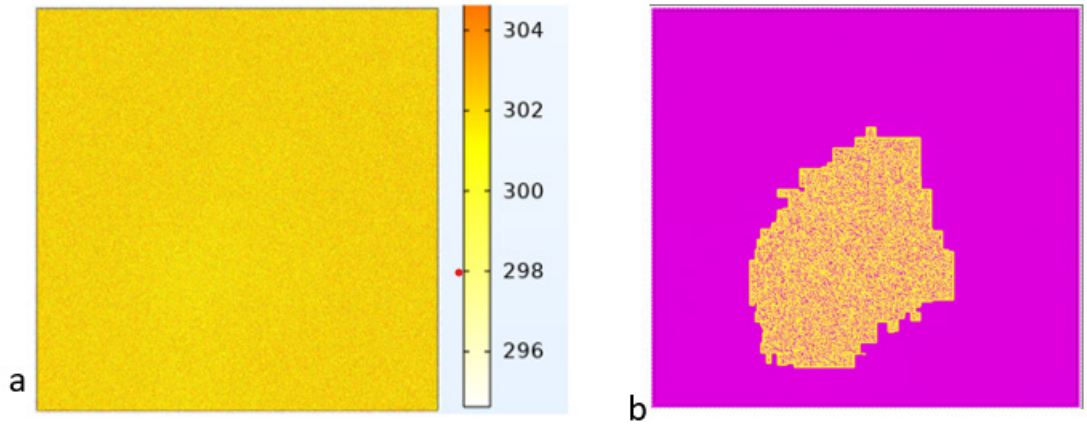

Figure 6. Thermogram obtained from simulation at t=30 sec a) before post processing b) after post processing.

3.2 Deep learning algorithm

The numerical experiments were repeated with various crack dimensions, and the location and depth of the crack were varied to prepare a dataset. The obtained datasets were trained using U-Net, a state of the art algorithem of deep learning. To evaluate the detection performance, F1 score was used in this study, which can be obtained as:

$$F1 = \frac{\frac{1}{2}\text{recall}\times\text{precision}}{precision+recall} \quad (4)$$

Here, the ratio of correctly recognised pixels to all detected pixels, including erroneous detection, can be used to derive the precision value. The recall value was calculated as the proportion of correctly recognised pixels to pixels in actual objects. From table 2, it can be seen that the precision, recall and F1 score are substantially good in this algorithm to detect even microlevel cacks. Figure 8 illustrates the crack detected through U-Net algorithm.

Table 2. Performance of U-Net algorithm.

	precision	*recall*	F1
U-Net	70.89%	81.82%	75.96%

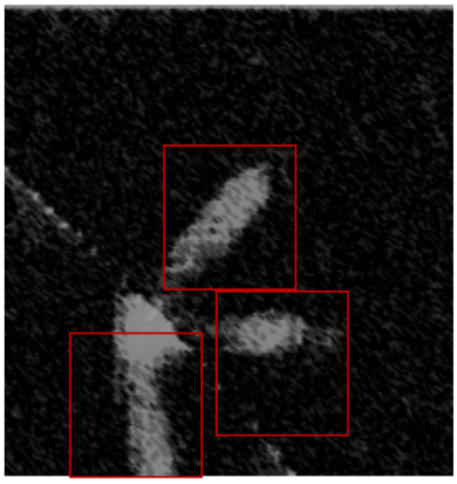

Figure 8. Crack detection after applying U-Net algorithm.

4 CONCLUSION

In this work, the feasibility of active thermography to detect the subsurface microcracks coalescence zone in a noisy environment has been assessed. A state-of the art deep learning algorithem U-Net has also introduced to automate the detection process such that objectivity can be obtained in the proposed method.

The following conclusions could be obtained:

1) Thermography survey of a rockmass based on solar radition is a time taking procedure as, obtaining one heating and cooling profile takes a whole day and night at a single location. From the present study it has been found that external heat stimuls as sinosoidal wave, is efficient and reliable.
2) The proposed post processing method in this study is quite efficient in reducing the noises arises due to non-uniform heating.
3) The U-Net algorithm was trained and verified on a dataset of 800 thermograms with cracks in various patterns. The algorithm satifactoraly detected and located the crack zone with good precision, recall, and F1 scores of 70.89%, 81.82%, and 74.96%, respectively.

REFERENCES

Budiansky, Bernard, and Richard J. O'connell. "Elastic moduli of a cracked solid." International journal of Solids and structures 12.2 (1976): 81-97.

Delle Piane, Claudio, et al. "Micro-crack enhanced permeability in tight rocks: An experimental and microstructural study." Tectonophysics 665 (2015): 149-156.

Griffiths, L., et al. "Quantification of microcrack characteristics and implications for stiffness and strength of granite." International Journal of Rock Mechanics and Mining Sciences 100 (2017): 138-150.

Guerin, Antoine, et al. "Detection of rock bridges by infrared thermal imaging and modeling." Scientific reports 9.1 (2019): 1-19.

He, M. C., J. L. Miao, and J. L. Feng. "Rock burst process of limestone and its acoustic emission characteristics under true-triaxial unloading conditions." International Journal of Rock Mechanics and Mining Sciences 47.2 (2010): 286-298.

He, Shengquan, et al. "Precursor of spatio-temporal evolution law of MS and AE activities for rock burst warning in steeply inclined and extremely thick coal seams under caving mining conditions." Rock Mechanics and Rock Engineering 52 (2019): 2415-2435.

Luodes, Hannu. "Natural stone assessment with ground penetrating radar." Estonian Journal of Earth Sciences 57.3 (2008): 149-155.

Lu, Cai-Ping, et al. "Microseismic low-frequency precursor effect of bursting failure of coal and rock." Journal of Applied Geophysics 79 (2012): 55-63.

Li, Xuelong, et al. "Rock burst monitoring by integrated microseismic and electromagnetic radiation methods." Rock Mechanics and Rock Engineering 49 (2016): 4393-4406.

Miao, Sheng-Jun, et al. "Rock burst prediction based on in-situ stress and energy accumulation theory." International Journal of Rock Mechanics and Mining Sciences 83 (2016): 86-94.

Poisson, Jérôme, et al. "Geophysical experiments to image the shallow internal structure and the moisture distribution of a mine waste rock pile." Journal of Applied Geophysics 67.2 (2009): 179-192.